Simultaneous regulation of antenna size and photosystem I/II stoichiometry in *Arabidopsis thaliana*

Authors:
Ting Jia[1], Hisashi Ito[1, 2], Ayumi Tanaka[1, 2]

Author affiliations:
[1]Institute of Low Temperature Science, Hokkaido University, N19 W8, Kita-ku, Sapporo, 060-0819, Japan
[2]CREST, Japan Science and Technology Agency, N19 W8, Kita-ku, Sapporo, 060-0819, Japan

Corresponding author:
Hisashi Ito
Institute of Low Temperature Science, Hokkaido University, N19 W8, Kita-ku, Sapporo, 060-0819, Japan
Tel: +81-11-706-5496
Fax: +81-11-706-5493
E-mail: ito98@lowtem.hokudai.ac.jp

Main conclusion

The photosystem I/II ratio increased when antenna size was enlarged by transient induction of CAO in chlorophyll *b*-less mutants, thus indicating simultaneous regulation of antenna size and photosystem I/II stoichiometry.

Abstract

Regulation of antenna size and photosystem I/II stoichiometry is an indispensable strategy for plants to acclimate to changes to light environments. When plants grown in high-light conditions are transferred to low-light conditions, the peripheral antennae of photosystems are enlarged. A change in the photosystem I/II ratio is also observed under the same light conditions. However, our knowledge of the correlation between antenna size modulation and variation in photosystem I/II stoichiometry remains limited. In this study, chlorophyll *a* oxygenase was transiently induced in *Arabidopsis thaliana* chlorophyll *b*-less mutants, *ch1-1*, to alter the antenna size without changing environmental conditions. In addition to the accumulation of chlorophyll *b*, the levels of the peripheral antenna complexes of both photosystems gradually increased, and these were assembled to the core antenna of both photosystems. However, the antenna size of photosystem II was greater than that of photosystem I. Immunoblot analysis of core antenna proteins showed that the number of photosystem I increased, but not that of photosystem II, resulting in an increase in the photosystem I/ II ratio. These results clearly indicate that antenna size adjustment was coupled with changes in photosystem I/II stoichiometry. Based on these results, the physiological importance of simultaneous regulation of antenna size and photosystem I/II stoichiometry is discussed in relation to acclimation to light conditions.

Keywords

chlorophyll *a* oxygenase

chlorophyll *b*

peripheral antenna complexes

photosystem reassembly

photosystem stoichiometry

Introduction

The survival of plants relies on solar energy, and photosynthesis is the only biological process that can harvest this energy. However, plants cannot escape from environmental changes, which directly affect photosynthetic reactions. To protect against environmental stress and to maintain optimal photosynthetic efficiency, plants have developed acclimation mechanisms. One of these mechanisms involves the photo-excitation balance between two photosystems through the modulation of photosynthetic apparatus. Regulation of the photosynthetic apparatus is dependent on two time-scales of acclimation; the short-term response, which rearranges the structure of the two photosystems to modulate light absorption (Wilhelm et al. 1989), and the long-term response, which re-adjusts photosynthetic stoichiometry (Dietzel et al. 2008) and modulates antenna size (Webb and Melis 1995). The short-term response occurs in seconds or minutes, meaning there is insufficient time to synthesize new chlorophyll-proteins or electron transport proteins, while the longer-term response occurs in hours or days and involves the synthesis and assembly of new membrane components and the degradation of other components (Anderson and Andersson 1988). Plants have developed complicated networks that mediate these time-sensitive responses to adapt to changing habitats.

The best documented evidence for the short term-response has come from studies investigating reversible phosphorylation (Anderson and Andersson 1988). A mobile pool of light-harvesting complexes (LHCs) serves as a switch to modulate the size of light-harvesting antenna in order to balance excitation energy between photosystem I (PSI) and photosystem II (PSII). This is known as a state transition and involves the movement of a portion of phosphorylated/de-phosphorylated LHCII molecules (Takahashi et al. 2006). When the reduced plastoquinone (PQ) pool reduces the cytochrome b_6f (cyt b_6f) complex, a redox sensitive kinase (STN7) is activated, which subsequently phosphorylates the mobile LHCII (Bellafiore et al. 2005; Depege et al. 2003), resulting in the detachment of LHCII from PSII and its association with PSI. In contrast, when the PQ pool is oxidized, another redox sensitive phosphatase (PPH1/TAP38) is activated, which subsequently de-phosphorylates the LHCII inducing re-association of the LHCII with PSII (Pribil et al. 2010; Shapiguzov et al. 2010). Signals indicating the redox state of the PQ pool trigger a state transition, which mediates a change in the antenna size of two photosystems in order to re-balance the excitation energy between two photosystems.

Non-photochemical quenching (NPQ) is another important short-term method of acclimation to high-light stress (Niyogi et al. 1998). The function of NPQ is to prevent plants from photo-damage by dissipating excess solar energy as heat via light-harvesting antenna in higher plants and green algae (Horton et al. 1996; Kulheim et al. 2002). NPQ occurs in the LHCII (Bonente et al. 2008), and down-regulation of NPQ was observed in the *Arabidopsis* mutant *ch1-1*, which retains only a minor light-harvesting complex component, Lhcb5, among 10 light-harvesting complexes (Havaux et al. 2007). NPQ is coupled to state transition via the STN7 kinase in the control of the chloroplast redox balance in fluctuating light conditions (Tikkanen et al. 2011).

State-transition is a tentative mechanism permitting acclimation to an immediate change in the light environment. When plants need to alter the excitation balance between the two photosystems for a long period, photosystems are newly synthesized or degraded to fit to a new environment. This adjustment of photosystem stoichiometry begins when imbalances in excitation are perceived via reduction/oxidation (redox) signals from the photosynthetic electron transport chain, and this process occurs over hours and days (Anderson et al. 1995; Fujita 1997; Melis et al. 1996).

Adjustment of the stoichiometry of the two photosystems is a common regulatory mechanism that counteracts the imbalance in excitation energy from cyanobacteria (Fujita 1997) to land plants (Fan et al. 2008). This adjustment is

regulated by a signal from the redox state of the PQ pool, which controls the synthesis of PSI core proteins (Fujita 1997). Variation in the stoichiometry of the two photosystems occurs due to the spectral quality (Myers et al. 1980) and intensity (Kawamura et al. 1979) of the light environment, and contributes an improvement in photosynthetic efficiency under various light conditions (Chow et al. 1990; Fujita et al. 1985; Murakami and Fujita 1991).

Regulation of antenna size by the de novo synthesis and degradation of peripheral antenna complexes is another important mechanism of long-term acclimation. In green plants, the antenna size of PSII is determined by LHCII, which is associated with the PSII core complex. Under low-light conditions, chlorophyll *b* synthesis is activated and the LHCII level increases resulting in a large antenna size. In contrast, LHCII must be decreased under high-light conditions in order to reduce antenna size and protect against high-light stress (Sato et al. 2015). To deal with fluctuating light environment, *LHC* genes are translationally regulated in response to light conditions (Floris et al. 2013). From a structural view point, it might be difficult to change the antenna size of both photosystems equally, because contribution of peripheral antenna is smaller in PSI than in PSII. Therefore, changes in the antenna size should be accompanied by the imbalance of excitation between the two photosystems which suggests that the regulation of antenna size and adjustment of PSI/PSII stoichiometry must occur simultaneously. However, the relationship between the regulation of antenna size and adjustment of photosystem stoichiometry has not well been examined.

Chlorophylls *a* and *b* are indispensable for the stabilization of LHC proteins in land plants (Plumley and Schmidt 1995) and *Chlamydomonas reinhardtii* (Polle et al. 2000). Indeed, the LHCII trimer is absent in the *Arabidopsis ch1* mutant, which does not accumulate chlorophyll *b* due to mutation of the *chlorophyll a oxygenase* (*CAO*) gene (Espineda et al. 1999; Tanaka et al. 1998). In this mutant, most of the peripheral antenna components (LHCII and LHCI) are present at extremely low levels, resulting in a small antenna size (Kim et al. 2009; Takabayashi et al. 2011). In order to examine the relationship between the regulation of antenna size and adjustment of PSI/PSII stoichiometry, *CAO* expression was transiently induced in the *ch1-1* mutant by which the antenna size can be altered without changing light condition. We observed a gradual increase in the PSI/PSII ratio concomitant to the increase in antenna size. We discuss the relationship between antenna size regulation and the adjustment of PSI/PSII stoichiometry.

Materials and methods

Plasmid construction and plant transformation

To transform *Arabidopsis*, a full-length coding sequence of the *Arabidopsis CAO* gene (AT1g44446) was introduced into the Gateway entry vector pENTR4 Dual (Invitrogen) and then introduced into the Gateway-compatible inducible vector pOpON, which was constructed from pOpOff2 (Craft et al. 2005; Wielopolska et al. 2005) by removing the antisense fragments with the restriction enzymes *Kpn*I and *Xba*I. The primer set used for transgenic plasmids (*CAO*-pENTR4) was as follows: forward 5'-CAAAAAAGCAGGCTCCACATGAACGCCGCCGTGTTTAGTCCTT-3', reverse 5'-AGAAAGCTGGGTCTAGATTTAGCCGGAGAAAGGTAGTTTATCATCGC-3'. Transgene expression was driven by the pOp6 promoter. The construct was introduced into *Agrobacterium tumefaciens* (strain GV3101) and transformed into the *Arabidopsis* mutant *ch1-1* (*CAO* deficient mutant) using a floral dip method (Clough and Bent 1998). Homozygous over-expressing transformants were screened by kanamycin resistance.

Plant materials and growth conditions

Arabidopsis thaliana WT (*Columbia*) and transgenic plants were grown at 25°C under continuous light conditions in chambers equipped with white fluorescent lamps at a light intensity of 80 µmol photons m^{-2} s^{-1}. *ch1-1* (CS3119) was obtained from the Arabidopsis Biological Resource Center. Four-to-five-week-old transformed plants were sprayed with 20 µM dexamethasone (Dex) to transiently induce *CAO* expression. Fully expanded rosette leaves from 4-week-old WT and from 4-to-5-week-old transformants with and without Dex treatment were harvested for use in these experiments. *CAO* mRNA levels were measured instead of CAO protein levels after Dex treatment, because CAO protein is under detectable levels by immunoblotting analysis (Yamasato et al. 2005). To examine the substrate of CAO, plants were grown on Murashige-Skoog (MS) agar under 16 h light/8 h dark conditions for 20 days, transferred to MS agar containing 20 µM Dex, and immediately placed in complete darkness for 5 days.

Pigment analysis

Leaves were weighed and ground in pure acetone cooled at -20°C using a Shaker Master (Biochemical Science) (Hu et al. 2013). The vessel used for grinding was also pre-cooled in liquid nitrogen. The extracts were centrifuged at 20 000 *g* for 10 min at 4°C. Chlorophylls *a* and chlorophyll *b* were analyzed by HPLC with a Symmetry C8 column (150-mm long, 4.6-mm inner diameter) (Waters) as previously described (Zapata et al. 2000). Elution profiles were monitored by measuring with a photodiode array (SPD-M10AVP, Shimadzu). Elution of chlorophyll *a* and chlorophyll *b* was monitored by checking absorbance at 664 and 648 nm, respectively. The chlorophyll content was quantified as the area of the chromatographic peak. The pure chlorophyll *a* and chlorophyll *b* were used to obtain the calibration slopes representing the area of the peak.

RNA extraction and quantitative real time-PCR (qRT-PCR) assay

Total RNA was extracted from leaf tissues of WT plants and plants treated with Dex for 0, 6, 12, and 24 hours using the RNeasy Mini Kit (Qiagen) according to the manufacturer's instructions. Leaf tissues were collected from fully expanded rosettes. The samples were used to synthesize cDNA using the Prime Script RT reagent kit with gDNA eraser (TaKaRa). qRT-PCR was performed using a Bio-Rad iQ5 real-time detection system (Bio-Rad). Primers used for qRT-PCR assays were as follows: for *CAO*, forward 5'- TCTGTGGAGACATTTCGCTG-3' and reverse 5'-AGTCTATACCGAACTCCGAGC-3'; for *ACT2*, forward 5'-ATTGTGCTCAGTGGTGGAAC-3' and reverse 5'-CGATTCCTGGACCTGCCTCA-3'. The *ch1-1* mutant has a 31 bp deletion (5'-AATTTAAACCACCGTGTATTGTTTTATCGAC-3') in the 8th exon of the *CAO* gene that leads to a truncated CAO protein (Oster et al. 2000). The *CAO* forward primer is at the end of the 8th exon and is not overlapped with the deleted region. The *CAO* reverse primer is at the 9th exon. The *ACT2* primers are at the 2nd exon and the 3' untranslated region, respectively. The reaction solution contained the cDNA template (all cDNA templates were diluted 100 times), primer pairs, SYBR Premix Ex Taq II (2×) (Takara), and sterilized distilled water. The exact volume added of each component followed the qRT-PCR protocol for SYBR Premix Ex Taq II. qRT-PCR was performed for 40 cycles. Microarray analysis was performed using the Arabidopsis Gene Expression Microarray kit (4X44K, V3) (Agilent) with RNA extracted from leaf tissues from plants treated with Dex treated for 0, 1, 2, and 4 days.

SDS-PAGE and immunoblot analysis

For total protein extraction, the leaf tissues were weighed, ground in liquid nitrogen, and homogenized with protein extraction buffer, which contained 125 mM Tris-HCl (pH 6.8), 4% (w/v) SDS, 10% (w/v) sucrose, and 10% (v/v) 2-mercaptoethanol. One-milligram leaf tissue was homogenized in 10 µL extraction buffer. An equal volume of sample buffer, which contained 50 mM Tris-HCl (pH 6.8), 2 mM EDTA, 10% (w/v) glycerol, 2% SDS and 6% 2-mercaptoethanol, was added to the mixture. A total of 1.5 µL (for CP1, D1, CP43, CP47) and 2.5 µL (for Lhcb1–6, Lhca1–4) of supernatant was subjected to SDS-PAGE analysis, then transferred onto a polyvinylidene difluoride membrane (Hybond-P, GE-Healthcare). Anti-rabbit primary antibody against CP1 (diluted 1:10,000), D1 (diluted 1:15,000), D2 (diluted 1:15,000), CP43 (diluted 1:20,000), CP47 (diluted 1:20,000), Lhcb1–6 (diluted 1:5,000), Lhca1–4 (diluted 1:5,000) were used for immunoblotting analysis. Antibodies were purchased from Agrisera except for CP1 and CP43 (Tanaka et al. 1991). Experiments were performed as described by Jia *et al*. (Jia et al. 2015). CP1 and CP43 were quantified using IMAGE J software (NIH). Serial dilutions of extracts from WT plants were used in every blotting analysis.

Blue-native PAGE analysis

Blue-native PAGE was performed as previously described (Takabayashi et al. 2011; Wittig et al. 2006). Purified thylakoid membranes (which contain 4.2 µg chlorophyll) were isolated from leaf tissues. Leaf tissues were homogenized using an ice-cooled glass homogenizer in grinding buffer containing 0.45 M sorbitol, 20 mM Tricine/KOH pH 8.4, 10 mM EDTA, 10 mM $NaHCO_3$ and 0.1% (w/v) BSA. Homogenates were filtered through a four-layer pore mesh, and then centrifuged at 4000 *g* at 4°C for 4 min. The supernatant was discarded and the pellet was washed twice with wash buffer containing 0.3 M sorbitol, 20 mM Tricine/KOH pH7.6, 5 mM $MgCl_2$, and 2.5 mM EDTA. The pellet was re-suspended in solubilization buffer containing 50 mM imidazole-HCl (pH 7.0), 20% glycerol, 5 mM 6-aminocaproic acid, and 1 mM EDTA, and was then mixed with 2% (w/v) α-dodecyl maltoside. After centrifugation at 20,000 *g* at 4°C for 5 min, supernatants were supplemented with 5% (w/v) CBB Serva Blue G, 500 mM 6-aminocaproic acid, and 50 mM imidazole-HCl (pH 7.0). Solubilized membrane proteins were separated on 4–14% acrylamide gradient gels.

Low temperature fluorescence measurement

Leaves were cut and immediately placed into glass tubes and then into liquid nitrogen. Fluorescence emission spectra were obtained at 77 K using a fluorescence spectrophotometer (F-2500, Hitachi). The wavelength of blue excitation was 465 nm with a slit width of 2.5 nm, and emission was obtained through a slit width 2.5 nm at a speed of 300 nm min^{-1}. Emission was monitored from 650 to 800 nm.

PSI and PSII antenna size measurements

Photo-oxidation and re-reduction of P700 in leaf tissues were examined using a pulse amplitude modification system (Dual-PAM-100, Walz), which included a dual wavelength (830/870 nm) unit or a single wavelength (730 nm) and was attached to a pulse amplitude modulation fluorometer. Leaves cut from plants were immediately illuminated in far-red

light until P700 was steadily oxidized to $P700^+$, then the observed maximum signal was used as the total amount of $P700^+$, and normalized to give the oxidation of the P700 fraction at any instant. According to a previous report (Kim et al. 2009), the time course of $P700^+$ could be fit using the following equation: $[P700^+] = e^{-Kred*t} + y_{ss}*(1-e^{-Kox*t})$, coefficient rate K_{ox} at constant far-red light indicates the relative antenna size of PSI.

Leaves were cut from plants and treated with 160 µM DCMU with 0.1% (w/v) Tween 20. Fluorescence was measured using a dual PAM system at actinic light intensity 5 (80 µmol photons m^{-2} s^{-1}) to assure maximal fluorescence yield. The fluorescence trace was normalized using the following equation: $Fv\ (t) = K_\alpha*A_{max}*(1–e^{-K\alpha*t})+ K_\beta*B_{max}*(1–e^{-K\beta*t})$ as described by Melis and Homann (Melis and Homann 1978). The fluorescence curve of PSII was consistent with two phases of the relative logarithmic area: the first and second linear phases (Greene et al. 1988). We used the Kα to indicate the relative antenna size of PSII.

Results

Transient induction of *CAO* expression and changes in the chlorophyll *a*/*b* ratio

CAO is a unique enzyme responsible for the synthesis of chlorophyll *b* (Tanaka et al. 1998), and the *cao* mutant *ch1-1* cannot synthesize chlorophyll *b*. In order to examine whether chlorophyll *b* is synthesized following transient expression of *CAO* in fully greened leaves of the *Arabidopsis ch1-1* mutant, we obtained three lines (line 6, 15, and 16) derived from the *ch1-1* mutant in which the *CAO* gene can be transiently induced by dexamethasone (Dex) treatment (see Materials and Methods). In these lines, chlorophyll *b* was not detected in the absence of Dex treatment suggesting that *CAO* was completely suppressed in these conditions. After 4 days of Dex treatment, HPLC analysis showed that chlorophyll *b* had successfully accumulated in all three lines, although the chlorophyll *a*/*b* ratios differed (Table 1). Line 6 had the lowest chlorophyll *a*/*b* ratio, indicating that this line most actively synthesized chlorophyll *b*. Therefore, line 6 was used for further experiments.

Figure 1 shows the changes in *CAO* mRNA levels in line 6 following Dex treatment. The *ch1-1* mutant significantly accumulated *CAO* mRNA. This mRNA might be a transcriptional product from the mutated *CAO* gene because the *ch1-1* mutant completely lacks chlorophyll *b*. After 6 hours of Dex treatment, the level of *CAO* mRNA in line 6 increased to levels higher than were observed in the WT plant, and gradually decreased but were retained at higher levels than in the WT.

Two substrates of CAO

Theoretically, two distinct pools of chlorophyll *a* could be used for chlorophyll *b* synthesis. One is the pre-existing chlorophyll *a* pool, which exists in chlorophyll-protein complexes such as CP47/CP43 and PSI core antenna. The other is newly synthesized chlorophyll *a* from glutamate. First, we examined whether pre-existing chlorophyll *a* can be a substrate for chlorophyll *b* synthesis. Plants were grown on agar medium under light conditions (16 h light/8 h dark) for 20 days, transferred to agar medium containing Dex, and immediately transferred to the dark. In the chlorophyll biosynthetic pathway, the conversion of protochlorophyllide *a* to chlorophyllide *a* is a light-dependent step catalyzed by light-dependent protochlorophyllide *a* oxidoreductase. When plants are incubated in darkness, this step is completely blocked and chlorophyll *a* is never synthesized. Therefore, pre-existing chlorophyll *a* is a unique substrate for

chlorophyll *b* synthesis under dark condition. Accumulation of chlorophyll *b* was observed following 5-days incubation with Dex in the dark (Fig. 2), indicating that pre-existing chlorophyll *a* in CP43/CP47 and/or PSI core antenna can be a substrate of CAO. However, the level of accumulated chlorophyll *b* was low, and the chlorophyll *a*/*b* ratio was 19. Only a small proportion of the pre-existing chlorophyll *a* was converted to chlorophyll *b*.

Next, we examined the time-course of chlorophyll *b* accumulation under light conditions, in which there is a continuous supply of newly synthesized chlorophyll (Fig. 3). After 12 hours of Dex treatment, chlorophyll *b* was detected consistent with the expression of *CAO*. The chlorophyll *b* content increased and the chlorophyll *a*/*b* ratio decreased up to 4 days. However, the chlorophyll *a*/*b* ratio (6.82) remained higher than that in the WT (4.13). Interestingly, the amount of chlorophyll *a* also increased, and this was accompanied by the accumulation of chlorophyll *b*. The total chlorophyll content increased by 50% following Dex treatment. This suggests that chlorophyll synthesis was upregulated in response to *CAO* expression. Glutamyl-tRNA reductase, which is encoded by *HemeA1* and catalyzes a step in the chlorophyll biosynthesis pathway, can be used to evaluate the activity of chlorophyll synthesis (Tanaka and Tanaka 2007). *HemeA1* gene expression determined by transcriptome analysis was enhanced 1.69 fold after 2 days of Dex treatment, consistent with the increase in chlorophyll content.

Accumulation of chlorophyll *b* and chlorophyll binding protein

Constitutive over-expression of *CAO* in *ch1-1* mutants can enhance the accumulation of LHC protein (Tanaka and Tanaka 2005). Here, we transiently induced *CAO* expression in *ch1-1* mutants and examined the accumulation of chlorophyll-binding proteins using immunoblotting. The results showed that the level of CP43 and D1 proteins did not significantly change in response to *CAO* expression, and the levels of these proteins were similar to those observed in the WT (Fig. 4). All of the LHC apoproteins were absent in the *ch1-1* mutant and gradually increased following Dex treatment, with the exception of Lhca2 and Lhcb5. These two proteins existed without chlorophyll *b* and were present at almost constant levels during Dex treatment. The level of CP1 protein was low in the mutant compared with the WT and increased during Dex treatment; after 4 days, and finally the level was almost equal to that observed in the WT.

In order to examine whether the increase in LHC proteins is accompanied by an increase in LHC mRNA, microarray analysis was carried out (Supplemental Fig. 1). The levels of Lhca1-4 and Lhcb1-6 mRNA did not change following Dex treatment. These results further confirm that *CAO* is involved in the regulation of LHC accumulation (Tanaka and Tanaka 2005).

NPQ is an effective short-term regulatory photo-protection process that can exert feedback control of excess light energy in PSII (Ruban et al. 2012). NPQ is made up of three components, qI, qT, and qE. qE, which is the major part of NPQ, develops and relaxes within seconds and/or minutes in high-light conditions (Horton and Ruban 1992; Krause and Weis 1991). qE quenching is thought to occur in the LHCII antenna. The *ch1-1* mutant displayed a low level of qE quenching (Supplemental Fig. 2). After Dex treatment, the level of NPQ was enhanced. Although the level of NPQ in Dex-treated plants was lower than that in the WT plants, the level of qE was consistent with the level of LHCII, suggesting that newly synthesized LHC in response to Dex treatment is functional. It is also known that despite an abundance of xanthophylls and PsbS, NPQ is small until chlorophyll *b* is synthesized in continuous light (Chow et al. 2000).

Accumulated LHC proteins assemble to form core antenna and integrated photosystems

Next, we investigated whether the newly synthesized LHC assembled with the core antenna as observed in the WT. First, we examined the formation of photosynthetic complexes using blue native polyacrylamide gel electrophoresis (PAGE) (Fig. 5). PSII dimers, PSII monomers and PSI monomers were observed, whereas PSII supercomplexes, PSI supercomplexes, and LHCII trimers did not accumulate in the *ch1-1* mutant, which is consistent with a previous report (Takabayashi et al. 2011). LHCII trimers and PSII-LHCII supercomplexes were detected after 1 day of Dex treatment, although the levels of these complexes were extremely low. Levels of LHCII trimers and PSII supercomplexes gradually increased up to 3 days of Dex treatment. These results indicate that newly synthesized LHCII trimers successfully associated with pre-existing PSII core complexes. The major LHCII proteins, Lhcb1-Lhcb3, exist in heterotrimeric forms whereas the minor LHCII proteins (Lhcb4-Lhcb6) exist in monomeric forms (Schmid 2008). The heterotrimeric LHCII proteins can associate with dimeric PSII core complexes via minor LHCII proteins, which function as linkers (Caffarri et al. 2009). Therefore it is reasonable that all of the LHCII apoproteins, including the minor LHC, accumulated and PSII-LHCII supercomplexes were formed in response to Dex treatment. These assembly processes are triggered solely by the induction of chlorophyll *b* synthesis.

Next, we measured the fluorescence emission spectra of PSII and PSI at liquid nitrogen temperatures. The wavelength of the peak fluorescence spectra of PSI was red-shifted from 725 to around 735 nm after Dex treatment. Simultaneously, the relative fluorescence intensity corresponding to PSI was increased, but remained lower than that of the WT (Fig. 6). Lhca1/4 and Lhca2/3 form red-emitting heterodimers (Wientjes and Croce 2011), which is consistent with the results obtained by immunoblotting showing that Lhca1 and Lhca4 were deficient and that Lhca3 was present at very low levels in *ch1-1* mutants. In the Lhca4 mutant, Lhca4 and Lhca1 were reported to be completely absent, less than 0.1% of Lhca2 and Lhca3 were detected, and the mutant exhibited red emission at around 720 nm. In Lhca1 mutants, the levels of Lhca2 and Lhca3 were consistent with those in the WT, but the levels of Lhca1 and Lhca4 were less than 0.1%, and the mutant exhibited red emission at around 732 nm (Ihalainen et al. 2005). In the present experiment, the red emission was observed at around 725 nm probably because of the low levels of Lhca1, Lhca3, and Lhca4 in *ch1-1*plants. Fluorescence corresponding to PSI in the *ch1-1* mutant might be partly derived from P700 and existing levels of Lhca2 and Lhca3. Red chlorophyll a603/a609 dimers have been reported to exist in each Lhca subunit (Qin et al. 2015) and contribute to low temperature fluorescence. It should be noted that fluorescence intensity also increased in response to Dex treatment, which might be caused by an increase in the level of PSI and/or the formation of Lhca containing red chlorophyll a603/a609. These results, together with immunoblotting analysis, clearly indicate that newly synthesized Lhca in response to Dex treatment successfully associated with PSI.

Newly synthesized peripheral antennae contribute to the increase in size

To evaluate the contribution of newly synthesized peripheral antennae to the antenna size of PSI and PSII, we measured the functional antenna size of photosystems using the dual PAM system. The rate coefficient of P700 photo-oxidation by steady far-red light was used to evaluate the relative antenna size of PSI as described in Materials and Methods. PSI antenna size of the *ch1-1* mutant was small compared to that of the WT. The antenna size increased in response to Dex treatment and was almost the same size as that in the WT after 2 days of Dex treatment (Fig. 7A).

The relative antenna size of PSII was measured by fluorescence induction using DCMU-poisoned green leaves. In a previous study, a fast exponential α-component and a slower exponential β-component were used to describe the primary

photochemistry of two types of PSII reaction centers; however, PSII corresponding to β-component ($PSII_\beta$) was reported to be inefficiently coupled to light-harvesting pigments with a small cross section for absorption (Melis and Homann 1978). Thus, in this experiment, we used the α-component to indicate the relative antenna size of PSII. K_α, corresponding to the $PSII_\alpha$ antenna size of the *ch1-1* mutant, was much smaller than that of the WT. This is consistent with the observation that major LHCII proteins were almost completely missing in the *ch1-1*mutant. K_α was gradually increased until 3 days of Dex treatment; however, the final level of K_α remained lower than that in the WT (Fig. 7B).

Accumulation of chlorophyll *b* induced changes in photosynthetic stoichiometry

A large portion of chlorophyll molecules belong to the core antenna in PSI; however, the peripheral antenna (LHCII) makes a large contribution to PSII. This indicates that the association of LHCII and LHCI with PSII and PSI core complexes, respectively, via the induction of chlorophyll *b* synthesis, induces the imbalance of excitation status between the two photosystems. However, the question then arises as to how the plant copes with this imbalance. To answer this, we measured the numbers of photosystems by measuring the levels of core antenna proteins and specific pigment of PSI and PSII. Figure 8 shows the changes in CP1 and CP43 protein levels during Dex treatment. The relative content of CP1 and CP43 was quantified by serial dilution (12.5, 25, 50, and 100%) (Fig. 8A). The results showed that the CP1 protein increased but the levels of CP43 protein were always constant when chlorophyll *b* synthesis was induced by Dex treatment (Fig. 8B). The ratio of CP1/CP43 was used to evaluate change of stoichiometry of the two photosystems. CP1/CP43 ratio was lower in *ch1-1* than in WT (Fig. 8C). The ratio was gradually increased during Dex treatment, but the ratio was still lower than in WT. This might be due to the low level of chlorophyll *b* compared to WT and antenna size could not increase to that of WT.

Discussion

Substrates of CAO

In this study, we show that there are two substrate pools for chlorophyll *b* synthesis; one includes the newly synthesized chlorophyll *a* and the other includes pre-existing chlorophyll *a* in the form of the pigment-protein complexes (Fig. 2). Previously, we reported that when greening cucumber cotyledons were treated with $CaCl_2$ in the dark, chlorophyll *a* bound to CP43 was converted to chlorophyll *b* followed by LHCII formation and CP43 degradation (Tanaka et al. 1991). In the present study, chlorophyll *b* synthesis was induced by *CAO* expression when chlorophyll synthesis was completely inhibited. This observation proves that both chlorophyll *a* and chlorophyllide *a* can serve the substrate for CAO. Considering that all chlorophyll exists in complexes with proteins, CAO might catalyze the conversion of chlorophyll *a*, which exists in chlorophyll-protein complexes. It has been reported that enzymes involved in chlorophyll metabolism can catalyze the conversion of not only free chlorophyll but also chlorophyll contained in complexes. For example, when isolated LHCII was incubated with chlorophyll *b* reductase (NOL), all the chlorophyll *b* in the complex was converted to 7-hydroxymethyl chlorophyll *a* (Horie et al. 2009). However, the chlorophyll *a*/*b* ratio was 19, even when the leaves were treated with Dex for 5 days, indicating that only 5% of total chlorophyll *a* was converted to chlorophyll *b*. At present, it is not known why only a limited amount of chlorophyll *a* was converted to chlorophyll *b* under dark condition. One possible reason is that CAO activity is down regulated in the dark, because CAO

utilizes ferredoxin, which is reduced by photosystems. In contrast, chlorophyll *b* was actively synthesized under the light condition and the chlorophyll *a*/*b* ratio fell to 5 (Fig. 3). Under the light condition, both newly synthesized and pre-existing chlorophyll *a* are substrates for chlorophyll *b* synthesis. This might be an important mechanism for the regulation of the LHC/reaction center ratio because this process contributes to the increase in LHC and to the decrease in the core antenna.

Another point of interest was that the total chlorophyll content was increased following the induction of *CAO* expression, indicating that chlorophyll biosynthetic activity was enhanced by CAO. This is consistent with a report that chlorophyll content was increased following the constitutive expression of CAO in tobacco (Biswal et al. 2012). Glutamyl-tRNA reductase (HemA1) catalyzes the committed step of chlorophyll synthesis, which is considered to be the most important regulatory step in chlorophyll synthesis. The level of *HemA1* mRNA was increased following the induction of *CAO* expression, which is consistent with the increase in the total chlorophyll content. However, the increase was small and further study is required to clarify the stimulating mechanism of chlorophyll synthesis by *CAO* expression.

Antenna size is regulated by *CAO* expression

Formation of peripheral antenna (LHC) is an important process for acclimation to light conditions because it determines the antenna size. The chlorophyll *a*/*b* ratio can be used as an index of antenna size because chlorophyll *b* exists only in peripheral antenna in land plants. The chlorophyll *a*/*b* ratio changes to adjust the antenna size in photosystems under various light intensities in *Arabidopsis* (Bailey et al. 2001). CAO is responsible for determining the chlorophyll *a*/*b* ratio and its expression is strictly regulated by light intensity. When high-light grown plants were transferred to low-light conditions, *CAO* expression was enhanced; by contrast, when low-light acclimated plants were transferred to high-light conditions, *CAO* expression was drastically decreased (Masuda et al. 2003). The following observations have led to the suggestion that chlorophyll *b* synthesis regulates the formation of the LHC. The barley chlorophyll *b*-less mutant (*chlorina*) lacked the majority of LHCs (Thornber and Highkin 1974) and the turnover rate of several LHC proteins increased (Bellemare et al. 1982). More specifically, the accumulation of LHC apoproteins (Lhcb1-Lhcb6 and Lhca1-Lhca4) was significantly reduced in this mutant (Krol et al. 1995). Bossman *et al.* reported that chlorophyll *b* levels correlated with LHC protein levels following the examination of 10 different alleles of *chlorina* (Bossmann et al. 1997), and a similar result was obtained with *Arabidopsis* (Takabayashi et al. 2011; Tzvetkova-Chevolleau et al. 2007). These results demonstrate the close relationship between chlorophyll *b* synthesis and LHC accumulation; however, it is not clear whether CAO activity regulates antenna size. Because light intensity affects various physiological processes, and the phenotype of *cao* mutant (*ch1-1*) plants includes not only deficiency in chlorophyll *b*, but also other phenotypes such as low growth rate and leaf thickness. In this study, we show that the accumulation of LHC was induced solely by *CAO* expression. Based on these experiments, we concluded that CAO activity primarily regulates the accumulation of LHC.

Under our experimental conditions, all the LHC proteins, except for Lhca2 and Lhcb5, were absent in the *ch1-1* mutant and were increased following the induction of *CAO*. Interestingly, mRNA levels of these Lhc proteins did not change as a result of altered *CAO* expression, which is consistent with the hypothesis that the expression level of CAO solely regulates the accumulation of LHC proteins, with the exception of Lhca2 and Lhcb5. The content of chlorophyll *b* in the complex does not account for its stability, because the chlorophyll *a/b* ratios in Lhca2 and Lhcb5 are 1.8 and 2,

respectively, which is lower than in other LHC complexes. The mechanism responsible for the stability of these complexes by chlorophyll *b* remains to be determined.

Simultaneous regulation of antenna size and adjustment of PSII/PSI stoichiometry

A working model is presented in Figure 9 showing that both antenna size and photosystem stoichiometry are concomitantly adjusted during photosystem restructure. Synthesized LHCs assembled with photosystems to form supercomplexes of both photosystems. Reestablished antennae of PSII were larger than those of PSI; therefore, PSI/PSII ratio increased to balance this situation.

Antenna size is altered according to changes in light intensity and quality. In green plants, antenna size is determined by the amount of LHCI and LHCII that are functionally associated with photosystems. If the antenna size of each photosystems changes to a different degree, the excitation status of both photosystems becomes unbalanced. However, equal increases in the antenna size of the two photosystems are difficult to achieve owing to structural differences in the light-harvesting systems of PSI and PSII. Therefore, it is reasonable to assume that the regulation of antenna size and the adjustment of PSI/PSII stoichiometry occur simultaneously. It is beneficial to use the *ch1-1* mutant to examine this hypothesis. It has been reported that major LHC proteins, Lhcb4, Lhcb5, Lhc6, Lhca1, Lhca2, Lhca3, and Lhca4 bind 14, 13, 9, 10, 14, 14, 15, and 15 chlorophyll molecules, respectively (Dekker and Boekema 2005; Qin et al. 2015). The core antenna of PSI and PSII bind 98 and 29 chlorophyll molecules, respectively. If we assume that the core antenna of PSI and PSII assemble with one copy of Lhca2 and Lhcb5, respectively, in the *ch1-1* mutant, the antenna sizes in PSI and II are calculated to contain 112 and 38 chlorophyll molecules, respectively. If we assume that two trimeric LHCIIs are associated with PSII and that four LHCIs (Lhca1-4) are associated with PSI, the antenna sizes of PSI and PSII are 156 and 146 chlorophyll molecules, respectively. Therefore, the difference in the PSI antenna size between *ch1-1* and WT is 1.4 fold and that of PSII is 3.8 fold. Overall these values are consistent with the antenna size measured by fluorescence, which was 1.25- and 2.2-fold larger of PSI and PSII antenna size, respectively, in WT compared to the *ch1-1* mutant. This indicates that if PSI/PSII stoichiometry is consistent between the WT and *ch1-1* plants, the level of excitation will be unbalanced. Therefore, the observation that the PSI/PSII ratio is lower in *ch1-1* than in WT is reasonable (Brestic et al. 2015; Kim et al. 1993). When chlorophyll *b* is synthesized and LHC accumulates, the antenna size might be preferentially increased in PSII as discussed. In fact, the PSI/PSII ratio immediately changed, and this was accompanied by an increase in antenna size. This clearly indicates that antenna size regulation and PSI/PSII stoichiometry occur simultaneously. This simultaneous regulation would contribute to or increase in the photosynthesis efficiency. Increase in quantum yield of O_2 evolution was observed when intermittently illuminated seedlings, which predominantly accumulated chlorophyll *a*, were transferred to continuous illumination where antenna size increased and PSII/PSI ratio decreased as observed in this study (Chow et al. 2000).

In cyanobacteria, the PSI/PSII ratio varied markedly depending on the quality of light. When the cells were grown under PSII light, the PSI/PSII ratio increased, whereas, under PSI light, the ratio decreased. Under these acclimation processes, only the levels of PSI changed, whereas those of PSII and cyt b_6f complex did not, suggesting that PSI is responsible for variation in the PSI/PSII ratio (Fujita 1997). This phenomenon was also observed in land plants, whose light-harvesting apparatus are quite different from those of cyanobacteria. The level of PSI changed but that of PSII did not when the antenna size was increased following the induction of chlorophyll *b*. A similar mechanism would operate between cyanobacteria and land plants.

Author contributions statement T.J., H.I. and A.T. conceived the original experiments; T.J. performed the experiments and wrote the manuscript; H.I. and A.T. supervised the experiments and the manuscript. A.T. is the principal investigator of the research grant.

Acknowledgments We thank Dr. Makio Yokono, Yukako Kato and Junko Kishimoto for technical assistance for antenna-size measurement. Finance of this study was provided by Core Research for Evolutional Science and Technology and the Japan Society for the Scientific Research 24370017 to A.T. T. J. was supported by a scholarship from China Scholarship Council.

Figure legends

Fig. 1 *CAO* mRNA expression level 0, 6, 12, and 24 hours after Dex treatment. Transcriptional level of *CAO* was analyzed by qRT-PCR. cDNA was prepared from total RNA extracted from fully expanded rosette leaves of line 6. The transcriptional level was normalized using *ACT2* as an internal housekeeping gene. Values are means and error bars represent ±SD (n = 4). Similar results were obtained from two independent experiments.

Fig. 2 HPLC elution profile of chlorophyll *a* and chlorophyll *b* extracts from Dex treated and untreated transformants. Traces were normalized to the peak of chlorophyll *a* at 648 nm.

Fig. 3 Analysis of chlorophyll levels before and after Dex treatment. Chlorophyll was extracted from fully expanded rosette leaves from WT and Dex treated and untreated CAO/*ch1-1* mutant plants. Error bars represents ± SD (n = 4).

Fig. 4 Immunoblotting analysis of LHC, PSI, and PSII core proteins. Total protein was extracted from fully expanded rosette leaves in WT and Dex treated and untreated *CAO*/*ch1-1* mutant plants. Protein samples were subjected to SDS-PAGE analysis. The experiment was repeated three times with similar results. The injection volume was normalized to the fresh-leaf weight.

Fig. 5 Analysis of protein complexes by blue native PAGE. A thylakoid membrane sample containing 4.2 µg chlorophyll was injected into each lane. After electrophoresis, the gel was stained with CBB.

Fig. 6 Low-temperature fluorescence measurements in leaves. The fluorescence emission spectra were measured with excitation at 465 nm. The curve was normalized at 695 nm.

Fig. 7 Measurement of functional antenna size of photosystem I and II. a Functional antenna size of photosystem I. Redox changes of $P700^{+}$ was obtained by applying a single turnover flash at 0 sec in steady far red light. Coefficient K_{ox} in formula $P700^{+} = e^{-K_{red}*t} + y_{ss} * (1-e^{-Kox*t})$ was use to indicate relative antenna size of PSI. b Functional antenna size of photosystem II. For relative antenna size of PSII, 40µM DCMU was used to inhibit electron transfer in $Q_{A,}$

photochemical fluorescence in PSII was examined and normalized using the formula: $Fv(t) = K\alpha * A_{max} * (1 - e^{-K\alpha * t}) + K_{\beta} * B_{max} * (1 - e^{-K\beta * t})$. Kα was used to indicate relative antenna size of PSII. Error bar represents ± SD (n=4). Independent experiment was repeated three times.

Fig. 8 Quantification of CP43 and CP1 protein levels. a SDS-PAGE and immunoblotting analysis. Membrane proteins extracted from leaves were subjected to SDS-PAGE and CP43 and CP1 were detected. The WT sample was used to generate a serial dilutions (100, 50, 25, and 12.5%) to quantify the relative content of CP43 and CP1. b Relative content of CP43 and CP1 in WT and Dex treated and untreated *CAO*/*ch1-1* mutant plants. c Ratio of PSI/PSII obtained from CP43/CP1. Error bar represents ± SD (n=4). Similar results were obtained from four independent experiments.

Fig. 9 Working model of PSI and II after CAO induction. a Primary distribution of PSI and PSII in *ch1-1* mutants before *CAO* induction. b After *CAO* was induced, LHCs assembled with PSI and PSII. Respectively, to form peripheral antenna and the peripheral antenna of PSII was larger than that of PSI. c To balance PSI and PSII excitation, there was an increase in PSI.

Supplemental data

Supplemental Fig. 1 Analysis of gene expression. Total RNA was extracted from fully expanded rosette leaves. An untreated sample was used as a control. Each dot corresponds to a gene on microarray.

Supplemental Fig. 2 Time course of non-photochemical quenching (qE type), Fo', Fm', and Fv'. Fully expanded leaves from WT and Dex treated and untreated *CAO*/*ch1-1* plants were incubated in the dark for 15 min. NPQ, Fm', Fo', and Fv' were then examined using the PAM system. Error bars represents ± SD (n = 3). Similar results were obtained from three independent experiments.

Reference

Anderson JM, Andersson B (1988) The dynamic photosynthetic membrane and regulation of solar energy conversion. Trends Biochem. Sci. 13: 351-355

Anderson JM, Chow WS, Park YI (1995) The grand design of photosynthesis: Acclimation of the photosynthetic apparatus to environmental cues. Photosynth. Res. 46: 129-139

Bailey S, Walters R, Jansson S, Horton P (2001) Acclimation of Arabidopsis thaliana to the light environment: the existence of separate low light and high light responses. Planta 213: 794-801

Bellafiore S, Barneche F, Peltier G, Rochaix J-D (2005) State transitions and light adaptation require chloroplast thylakoid protein kinase STN7. Nature 433: 892-895

Bellemare G, Bartlett SG, Chua NH (1982) Biosynthesis of chlorophyll a/b-binding polypeptides in wild type and the chlorina f2 mutant of barley. J. Biol. Chem. 257: 7762-7767

Biswal AK, Pattanayak GK, Pandey SS, Leelavathi S, Reddy VS, Govindjee, Tripathy BC (2012) Light Intensity-Dependent Modulation of Chlorophyll b Biosynthesis and Photosynthesis by Overexpression of Chlorophyllide a Oxygenase in Tobacco. Plant Physiol. 159: 433-449

Bonente G, Howes BD, Caffarri S, Smulevich G, Bassi R (2008) Interactions between the photosystem II subunit PsbS and xanthophylls studied in vivo and in vitro. J. Biol. Chem. 283: 8434-8445

Bossmann B, Knoetzel J, Jansson S (1997) Screening of chlorina mutants of barley (Hordeum vulgare L.) with antibodies against light-harvesting proteins of PS I and PS II: Absence of specific antenna proteins. Photosynth. Res. 52: 127-136

Brestic M, Zivcak M, Kunderlikova K, Sytar O, Shao H, Kalaji H, Allakhverdiev S (2015) Low PSI content limits the photoprotection of PSI and PSII in early growth stages of chlorophyll b-deficient wheat mutant lines. Photosynth. Res. 125: 151-166

Caffarri S, Kouril R, Kereiche S, Boekema EJ, Croce R (2009) Functional architecture of higher plant photosystem II supercomplexes. EMBO J. 28: 3052-3063

Chow WS, Funk C, Hope AB, Govindjee (2000) Greening of intermittent-light-grown bean plants in continuous light: thylakoid components in relation to photosynthetic performance and capacity for photoprotection. Indian J. Biochem. Biophys. 37: 395-404

Chow WS, Melis A, Anderson JM (1990) Adjustments of photosystem stoichiometry in chloroplasts improve the quantum efficiency of photosynthesis. Proceedings of the National Academy of Sciences 87: 7502-7506

Clough SJ, Bent AF (1998) Floral dip: a simplified method for Agrobacterium-mediated transformation ofArabidopsis thaliana. Plant J. 16: 735-743

Craft J, Samalova M, Baroux C, Townley H, Martinez A, Jepson I, Tsiantis M, Moore I (2005) New pOp/LhG4 vectors for stringent glucocorticoid-dependent transgene expression in Arabidopsis. Plant J. 41: 899-918

Dekker JP, Boekema EJ (2005) Supramolecular organization of thylakoid membrane proteins in green plants. Biochim. Biophys. Acta 1706: 12-39

Depege N, Bellafiore S, Rochaix JD (2003) Role of chloroplast protein kinase Stt7 in LHCII phosphorylation and state transition in Chlamydomonas. Science 299: 1572-1575

Dietzel L, Bräutigam K, Pfannschmidt T (2008) Photosynthetic acclimation: State transitions and adjustment of photosystem stoichiometry – functional relationships between short-term and long-term light quality acclimation in plants. FEBS J. 275: 1080-1088

Espineda CE, Linford AS, Devine D, Brusslan JA (1999) The AtCAO gene, encoding chlorophyll a oxygenase, is required for chlorophyll b synthesis in Arabidopsis thaliana. Proc. Natl. Acad. Sci. U. S. A. 96: 10507-10511

Fan D-Y, Hope AB, Smith PJ, Jia H, Pace RJ, Anderson JM, Chow WS (2008) The Stoichiometry of Photosystem II to Photosystem I in Higher Plants. In: Allen JF, Gantt E, Golbeck JH, Osmond B (eds) Photosynthesis. Energy from the Sun: 14th International Congress on Photosynthesis. Springer Netherlands, Dordrecht, pp 7-10

Floris M, Bassi R, Robaglia C, Alboresi A, Lanet E (2013) Post-transcriptional control of light-harvesting genes expression under light stress. Plant Mol. Biol. 82: 147-154

Fujita Y (1997) A study on the dynamic features of photosystem stoichiometry: Accomplishments and problems for future studies. Photosynth. Res. 53: 83-93

Fujita Y, Ohki K, Murakami A (1985) Chromatic Regulation of Photosystem Composition in the Photosynthetic System of Red and Blue-Green Algae. Plant Cell Physiol. 26: 1541-1548
Greene BA, Staehelin LA, Melis A (1988) Compensatory Alterations in the Photochemical Apparatus of a Photoregulatory, Chlorophyll b-Deficient Mutant of Maize. Plant Physiol. 87: 365-370
Havaux M, Dall'Osto L, Bassi R (2007) Zeaxanthin Has Enhanced Antioxidant Capacity with Respect to All Other Xanthophylls in Arabidopsis Leaves and Functions Independent of Binding to PSII Antennae. Plant Physiol. 145: 1506-1520
Horie Y, Ito H, Kusaba M, Tanaka R, Tanaka A (2009) Participation of chlorophyll b reductase in the initial step of the degradation of light-harvesting chlorophyll a/b-protein complexes in Arabidopsis. J. Biol. Chem. 284: 17449-17456
Horton P, Ruban AV (1992) Regulation of Photosystem II. Photosynth. Res. 34: 375-385
Horton P, Ruban AV, Walters RG (1996) REGULATION OF LIGHT HARVESTING IN GREEN PLANTS. Annu. Rev. Plant Physiol. Plant Mol. Biol. 47: 655-684
Hu X, Tanaka A, Tanaka R (2013) Simple extraction methods that prevent the artifactual conversion of chlorophyll to chlorophyllide during pigment isolation from leaf samples. Plant Methods 9: 19
Ihalainen JA, Klimmek F, Ganeteg U, van Stokkum IHM, van Grondelle R, Jansson S, Dekker JP (2005) Excitation energy trapping in photosystem I complexes depleted in Lhca1 and Lhca4. FEBS Lett. 579: 4787-4791
Jia T, Ito H, Hu X, Tanaka A (2015) Accumulation of the NON-YELLOW COLORING 1 protein of the chlorophyll cycle requires chlorophyll b in Arabidopsis thaliana. Plant J. 81: 586-596
Kawamura M, Mimuro M, Fujita Y (1979) Quantitative relationship between two reaction centersin the photosynthetic system of blue-green algae. Plant Cell Physiol. 20: 697-705
Kim E-H, Li X-P, Razeghifard R, Anderson JM, Niyogi KK, Pogson BJ, Chow WS (2009) The multiple roles of light-harvesting chlorophyll a/b-protein complexes define structure and optimize function of Arabidopsis chloroplasts: A study using two chlorophyll b-less mutants. Biochim. Biophys. Acta 1787: 973-984
Kim JH, Glick RE, Melis A (1993) Dynamics of Photosystem Stoichiometry Adjustment by Light Quality in Chloroplasts. Plant Physiol. 102: 181-190
Krause GH, Weis E (1991) Chlorophyll Fluorescence and Photosynthesis: The Basics. Annu. Rev. Plant Physiol. Plant Mol. Biol. 42: 313-349
Krol M, Spangfort MD, Huner N, Oquist G, Gustafsson P, Jansson S (1995) Chlorophyll a/b-Binding Proteins, Pigment Conversions, and Early Light-Induced Proteins in a Chlorophyll b-less Barley Mutant. Plant Physiol. 107: 873-883
Kulheim C, Agren J, Jansson S (2002) Rapid regulation of light harvesting and plant fitness in the field. Science 297: 91-93
Masuda T, Tanaka A, Melis A (2003) Chlorophyll antenna size adjustments by irradiance in Dunaliella salina involve coordinate regulation of chlorophyll a oxygenase (CAO) and Lhcb gene expression. Plant Mol. Biol. 51: 757-771
Melis A, Homann PH (1978) A selective effect of Mg2+ on the photochemistry at one type of reaction center in photosystem II of chloroplasts. Arch. Biochem. Biophys. 190: 523-530
Melis A, Murakami A, Nemson JA, Aizawa K, Ohki K, Fujita Y (1996) Chromatic regulation inChlamydomonas reinhardtii alters photosystem stoichiometry and improves the quantum efficiency of photosynthesis. Photosynth. Res. 47: 253-265
Murakami A, Fujita Y (1991) Steady State of Photosynthetic Electron Transport in Cells of the Cyanophyti Synechocystis PCC 6714 Having Different Stoichiometry between PS I and PS II: Analysis of Flash-Induced Oxidation-Reduction of Cytochrome f and P700 under Steady State of Photosynthesis. Plant Cell Physiol. 32: 213-222
Myers J, Graham JR, Wang RT (1980) Light Harvesting in Anacystis nidulans Studied in Pigment Mutants. Plant Physiol. 66: 1144-1149
Niyogi KK, Grossman AR, Bjorkman O (1998) Arabidopsis mutants define a central role for the xanthophyll cycle in the regulation of photosynthetic energy conversion. Plant Cell 10: 1121-1134
Oster U, Tanaka R, Tanaka A, Rudiger W (2000) Cloning and functional expression of the gene encoding the key enzyme for chlorophyll b biosynthesis (CAO) from Arabidopsis thaliana. Plant J. 21: 305-310
Plumley GF, Schmidt GW (1995) Light-Harvesting Chlorophyll a/b Complexes: Interdependent Pigment Synthesis and Protein Assembly. Plant Cell 7: 689-704

Polle JE, Benemann JR, Tanaka A, Melis A (2000) Photosynthetic apparatus organization and function in the wild type and a chlorophyll b-less mutant of Chlamydomonas reinhardtii. Dependence on carbon source. Planta 211: 335-344
Pribil M, Pesaresi P, Hertle A, Barbato R, Leister D (2010) Role of plastid protein phosphatase TAP38 in LHCII dephosphorylation and thylakoid electron flow. PLoS Biol. 8: e1000288
Qin X, Suga M, Kuang T, Shen J-R (2015) Structural basis for energy transfer pathways in the plant PSI-LHCI supercomplex. Science 348: 989-995
Ruban AV, Johnson MP, Duffy CDP (2012) The photoprotective molecular switch in the photosystem II antenna. Biochim. Biophys. Acta 1817: 167-181
Sato R, Ito H, Tanaka A (2015) Chlorophyll b degradation by chlorophyll b reductase under high-light conditions. Photosynth. Res. 126: 249-259
Schmid VH (2008) Light-harvesting complexes of vascular plants. Cell Mol Life Sci 65: 3619-3639
Shapiguzov A, Ingelsson B, Samol I, Andres C, Kessler F, Rochaix J-D, Vener AV, Goldschmidt-Clermont M (2010) The PPH1 phosphatase is specifically involved in LHCII dephosphorylation and state transitions in Arabidopsis. Proc. Natl. Acad. Sci. U. S. A. 107: 4782-4787
Takabayashi A, Kurihara K, Kuwano M, Kasahara Y, Tanaka R, Tanaka A (2011) The oligomeric states of the photosystems and the light-harvesting complexes in the Chl b-less mutant. Plant Cell Physiol. 52: 2103-2114
Takahashi H, Iwai M, Takahashi Y, Minagawa J (2006) Identification of the mobile light-harvesting complex II polypeptides for state transitions in Chlamydomonas reinhardtii. Proc. Natl. Acad. Sci. U. S. A. 103: 477-482
Tanaka A, Ito H, Tanaka R, Tanaka NK, Yoshida K, Okada K (1998) Chlorophyll a oxygenase (CAO) is involved in chlorophyll b formation from chlorophyll a. Proc. Natl. Acad. Sci. U. S. A. 95: 12719-12723
Tanaka A, Yamamoto Y, Tsuji H (1991) Formation of chlorophyll-protein complexes during greening 2. Redistribution of chlorophyll among apoproteins. Plant Cell Physiol. 32: 195-204
Tanaka R, Tanaka A (2005) Effects of chlorophyllide a oxygenase overexpression on light acclimation in Arabidopsis thaliana. Photosynth. Res. 85: 327-340
Tanaka R, Tanaka A (2007) Tetrapyrrole Biosynthesis in Higher Plants. Annu. Rev. Plant Biol. 58: 321-346
Thornber JP, Highkin HR (1974) Composition of the photosynthetic apparatus of normal barley leaves and a mutant lacking chlorophyll b. Eur. J. Biochem. 41: 109-116
Tikkanen M, Grieco M, Aro E-M (2011) Novel insights into plant light-harvesting complex II phosphorylation and ‘state transitions’. Trends Plant Sci. 16: 126-131
Tzvetkova-Chevolleau T, Franck F, Alawady AE, Dall'Osto L, Carriere F, Bassi R, Grimm B, Nussaume L, Havaux M (2007) The light stress-induced protein ELIP2 is a regulator of chlorophyll synthesis in Arabidopsis thaliana. Plant J. 50: 795-809
Webb MR, Melis A (1995) Chloroplast Response in Dunaliella salina to Irradiance Stress (Effect on Thylakoid Membrane Protein Assembly and Function). Plant Physiol. 107: 885-893
Wielopolska A, Townley H, Moore I, Waterhouse P, Helliwell C (2005) A high-throughput inducible RNAi vector for plants. Plant Biotechnol. J. 3: 583-590
Wientjes E, Croce R (2011) The light-harvesting complexes of higher-plant Photosystem I: Lhca1/4 and Lhca2/3 form two red-emitting heterodimers. The Biochemical journal 433: 477-485
Wilhelm C, Krämer P, Lenartz-Weiler I (1989) The energy distribution between the photosystems and light-induced changes in the stoichiometry of system I and II reaction centers in the chlorophyll b-containing alga Mantoniella squamata (Prasinophyceae). Photosynth. Res. 20: 221-233
Wittig I, Braun HP, Schagger H (2006) Blue native PAGE. Nat Protoc 1: 418-428
Yamasato A, Nagata N, Tanaka R, Tanaka A (2005) The N-terminal domain of chlorophyllide a oxygenase confers protein instability in response to chlorophyll b accumulation in Arabidopsis. Plant Cell 17: 1585-1597
Zapata M, Rodríguez F, Garrido JL (2000) Separation of chlorophylls and carotenoids from marine phytoplankton: a new HPLC method using a reversed phase C8 column and pyridine-containing mobile phases. Mar. Ecol. Prog. Ser. 195: 29-45

Figure 1

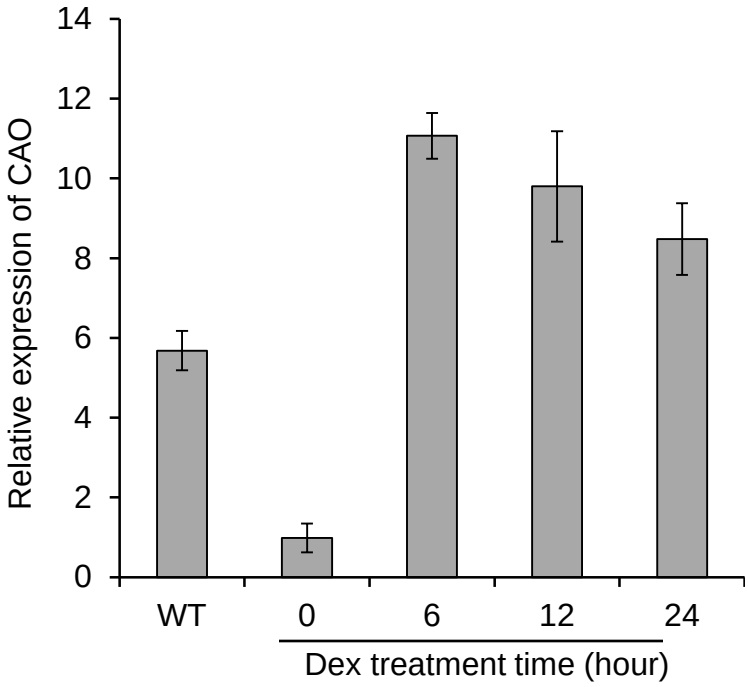

Fig. 1 *CAO* mRNA expression level 0, 6, 12, and 24 hours after Dex treatment. Transcriptional level of *CAO* was analyzed by qRT-PCR. cDNA was prepared from total RNA extracted from fully expanded rosette leaves of line 6. The transcriptional level was normalized using *ACT2* as an internal housekeeping gene. Values are means and error bars represent ±SD (n = 4). Similar results were obtained from two independent experiments.

Figure 2

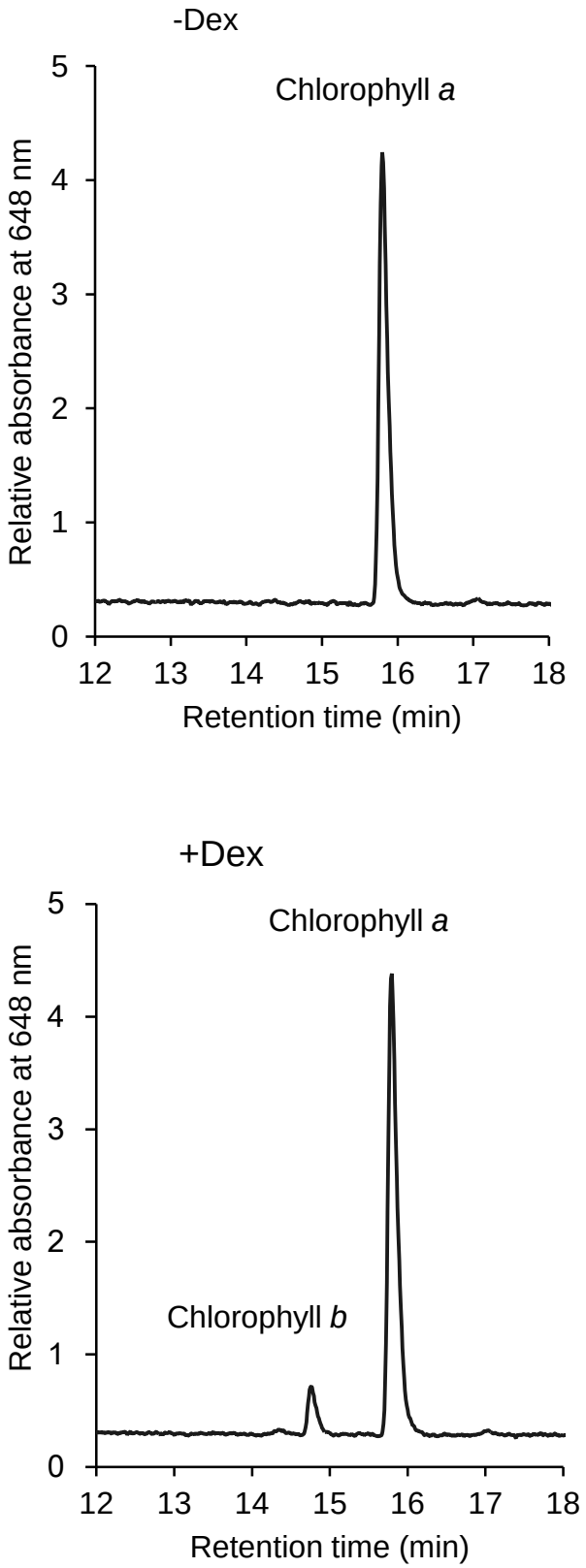

Fig. 2 HPLC elution profile of chlorophyll *a* and chlorophyll *b* extract from with/ without Dex treated transformants. Traces were normalized to the peak of chlorophyll *a* at 648nm.

Figure 3

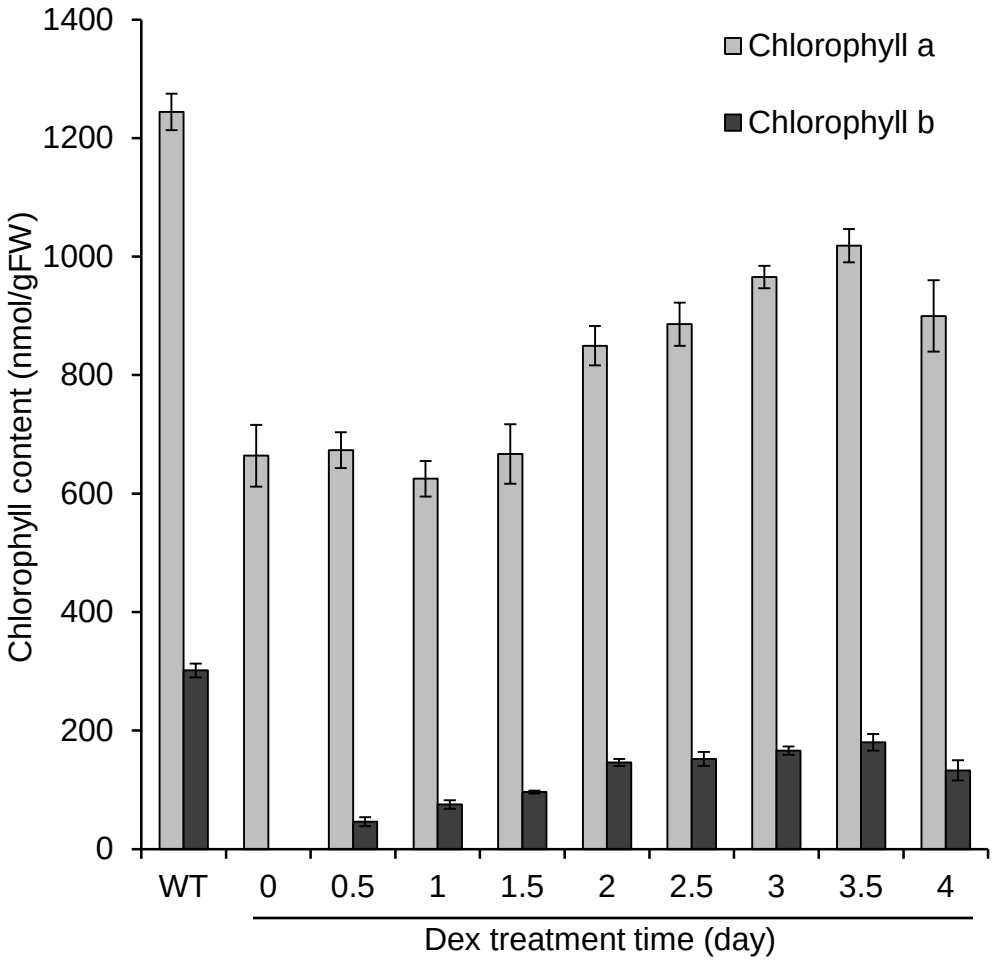

Fig. 3 Analysis of chlorophyll content before after Dex treatment. Chlorophyll was extracted from fully expanded rosette leaves in WT and with / without Dex treated CAO/*ch1-1.* Error bar represents ± SD (n=4).

Figure 4

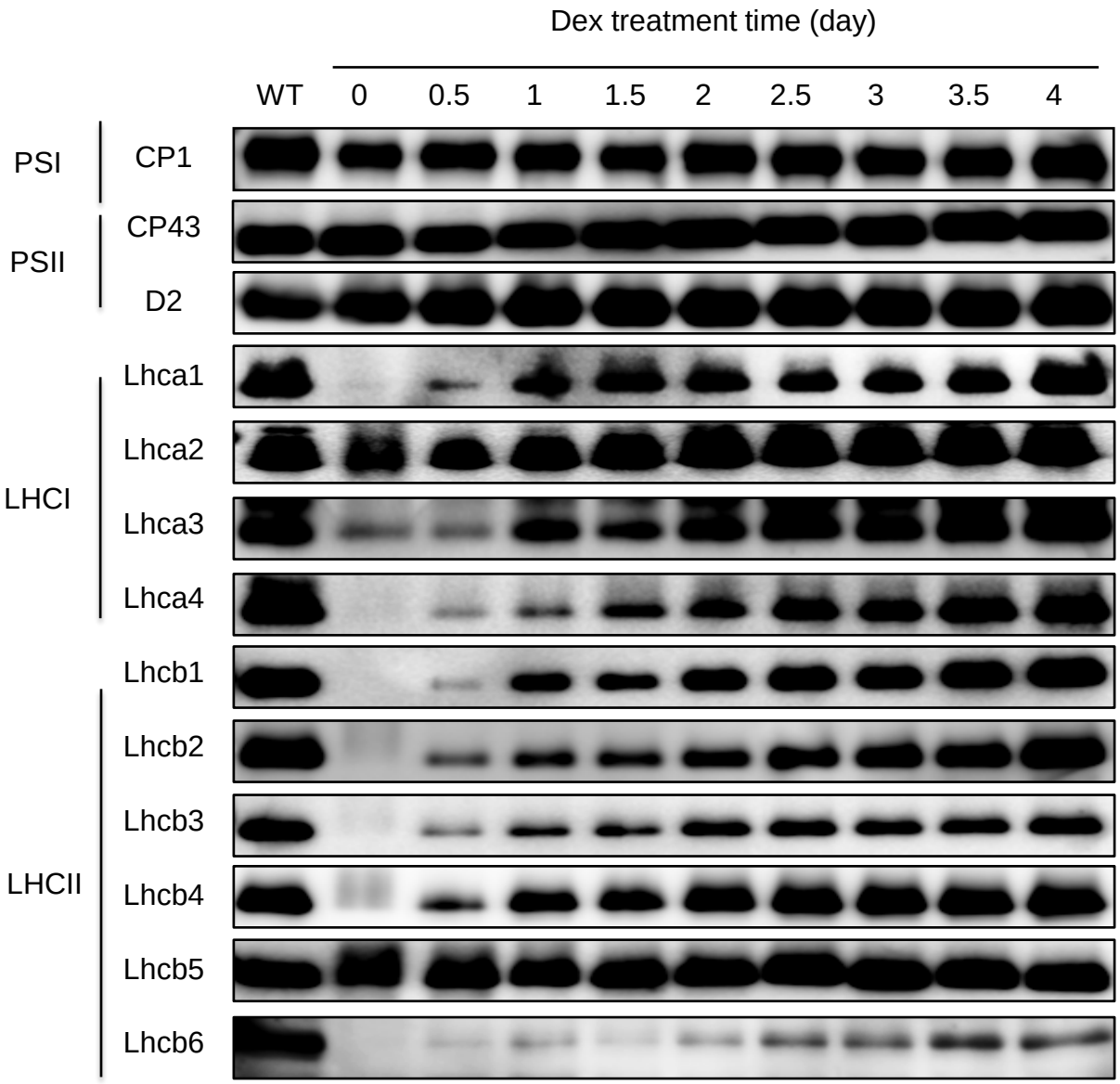

Fig. 4 Immunoblotting analysis of LHCs, PSI and PSII core proteins. Total protein was extracted from fully expanded rosette leaves in WT and with/without Dex treated *CAO*/*ch1-1*. Protein samples were subjected in SDS-PAGE and analyzed. The experiment were repeated three times with similar results. Injection volume was normalized by fresh leaf weight.

Figure 5

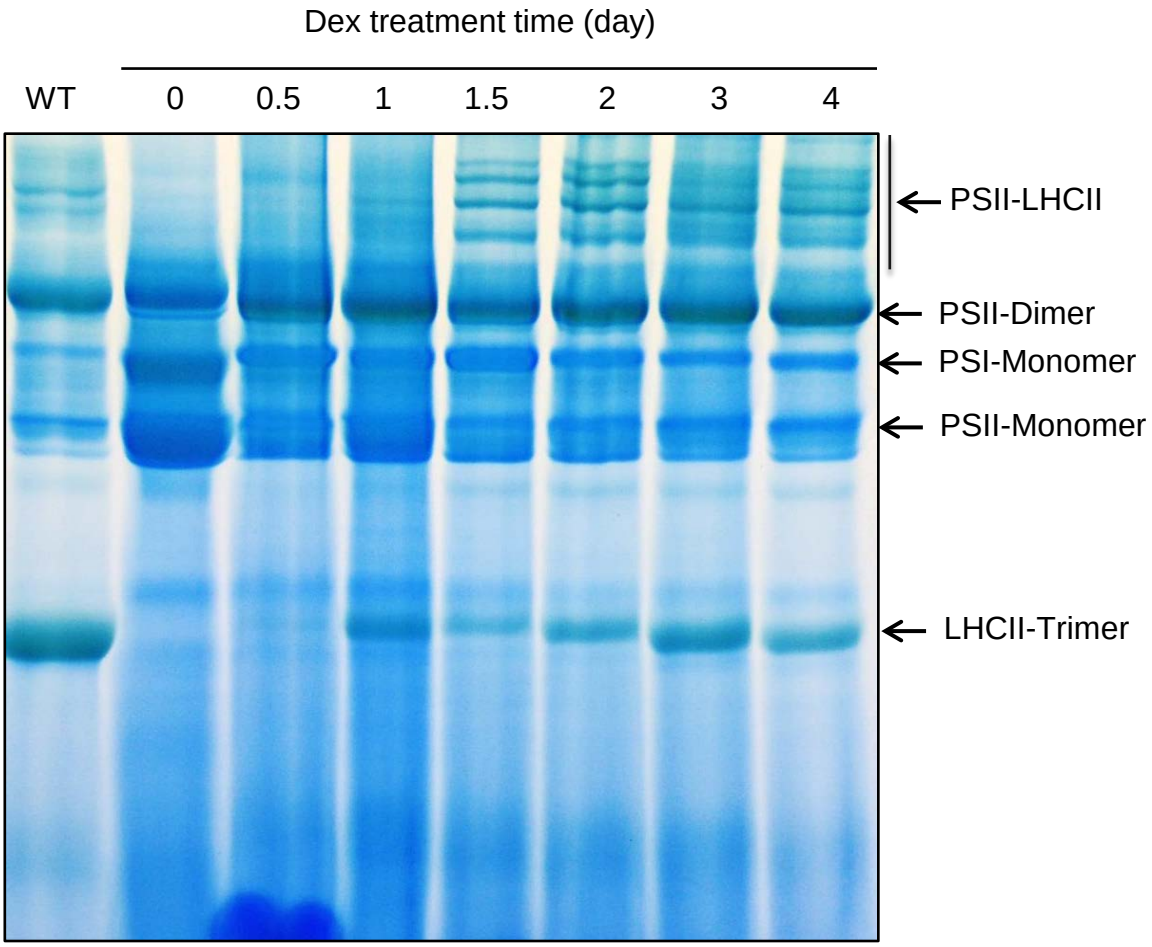

Fig. 5 Analysis of protein complexes. Thylakoid membrane containing 4.2 μg Chl was injected in each lane, after blue native PAGE, the gel was stained in CBB.

Figure 6

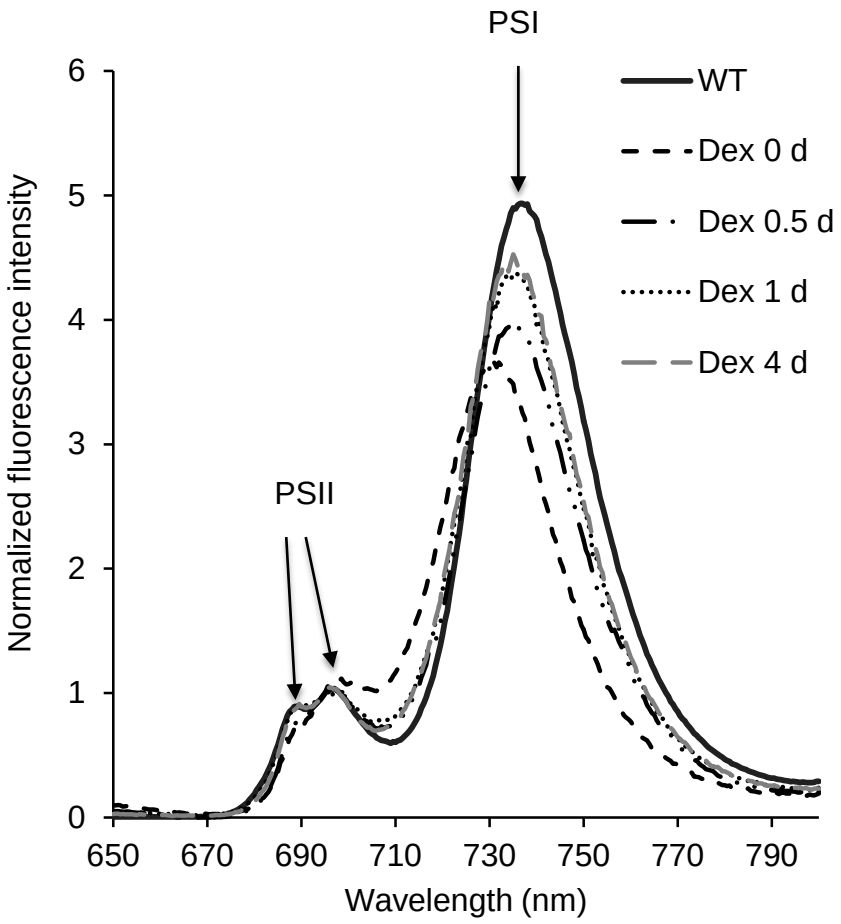

Fig. 6 Measurement of low temperature fluorescence. Fluorescence emission spectra were measured with excitation at 465 nm. The curve was normalized at 695nm

Figure 7

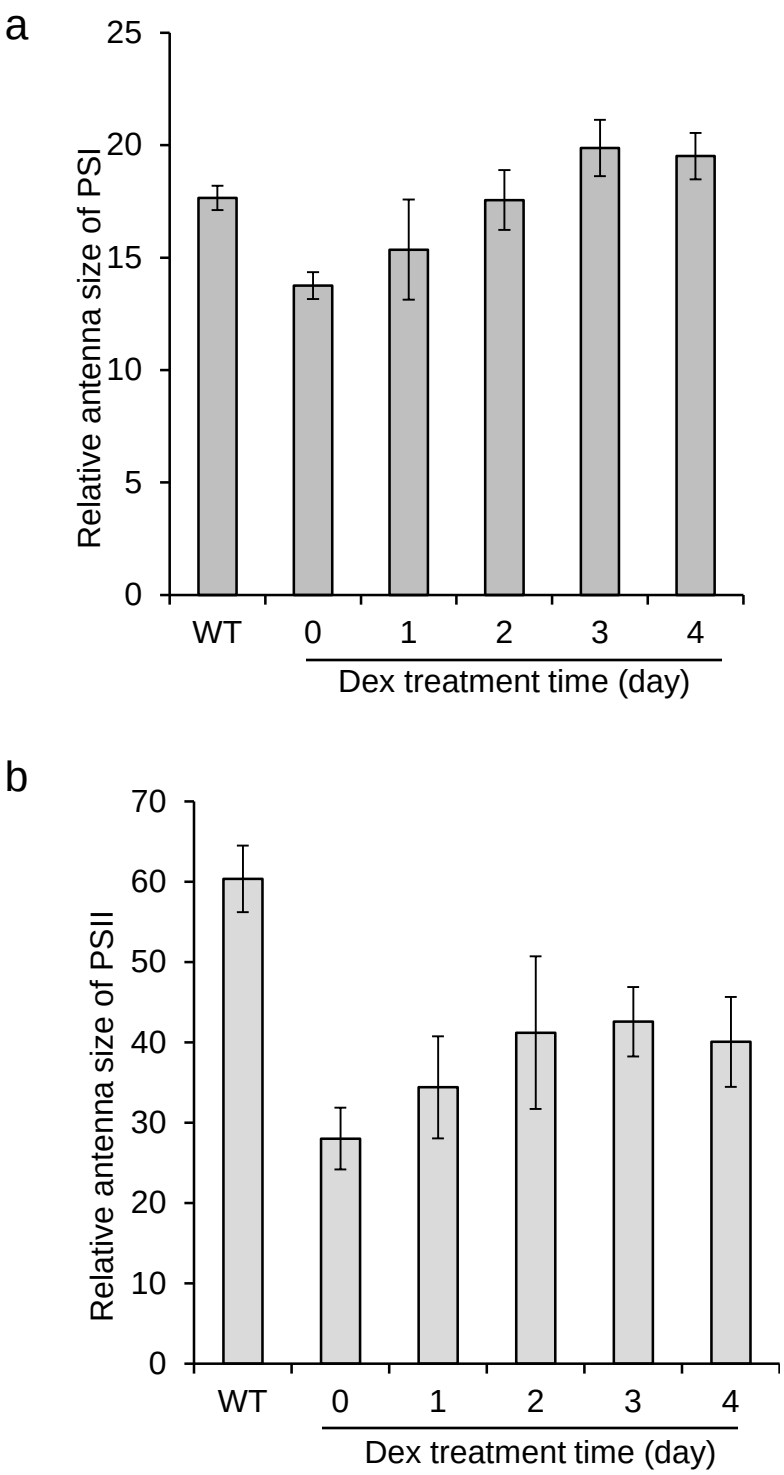

Fig. 7 Measurement of functional antenna size of photosystem I and II. a Functional antenna size of photosystem I. Redox changes of $P700^{+}$ was obtained by applying a single turnover flash at 0 sec in steady far red light. coefficient K_{ox} in formula $P700^{+}= e^{-Kred*t}+y_{ss}* (1-e^{-Kox*t})$ was use to indicate relative antenna size of PSI. b Functional antenna size of photosystem II. For relative antenna size of PSII, 40μM DCMU was used to inhibit electron transfer in $Q_{A,}$ photochemical fluorescence in PSII was examined and normalized using the formula: $Fv\ (t) = K\alpha*A_{max}*(1 – e^{-K\alpha*t})+ K_{\beta}*B_{max}*(1 – e^{-K\beta*t})$. Kα was used to indicate relative antenna size of PSII. Error bar represents ± SD (n=4). Independent experiment was repeated three times.

Figure 8

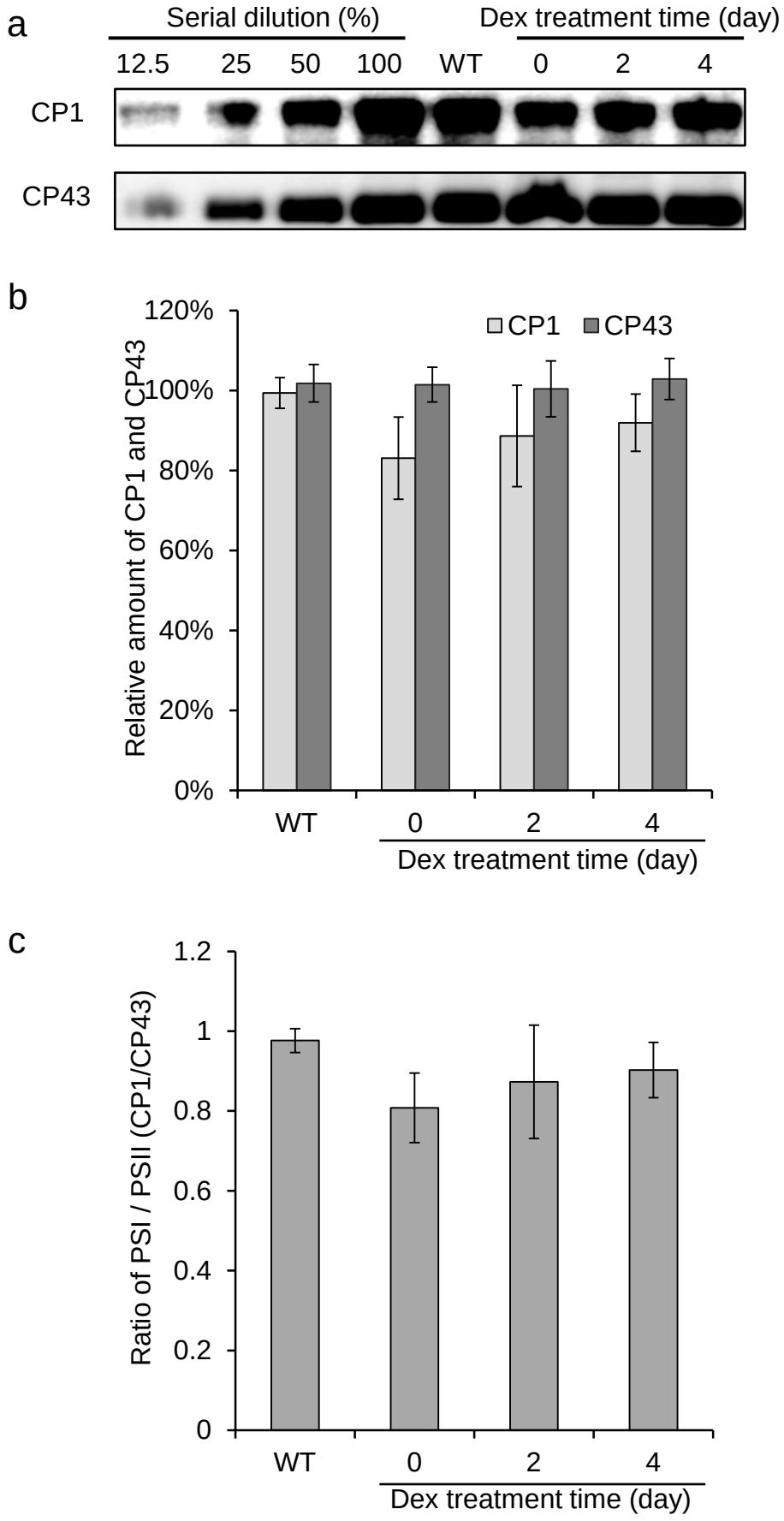
a
Serial dilution (%)
Dex treatment time (day)
12.5
25
50
100
WT
0
2
4
CP1
CP43
b
CP1
CP43
Relative amount of CP1 and CP43
120%
100%
80%
60%
40%
20%
0%
WT
0
2
4
Dex treatment time (day)
c
Ratio of PSI / PSII (CP1/CP43)
1.2
1
0.8
0.6
0.4
0.2
0
WT
0
2
4
Dex treatment time (day)

Fig. 8 Quantification of CP43 and CP1 protein levels. a SDS-PAGE and immunoblotting analysis. Membrane proteins extracted from leaves were subjected to SDS-PAGE and CP43 and CP1 were detected. The WT sample was used to generate a serial dilutions (100, 50, 25, and 12.5%) to quantify the relative content of CP43 and CP1. b Relative content of CP43 and CP1 in WT and Dex treated and untreated *CAO*/*ch1-1* mutant plants. c Ratio of PSI/PSII obtained from CP43/CP1. Error bar represents ± SD (n=4). Similar results were obtained from four independent experiments.

Figure 9

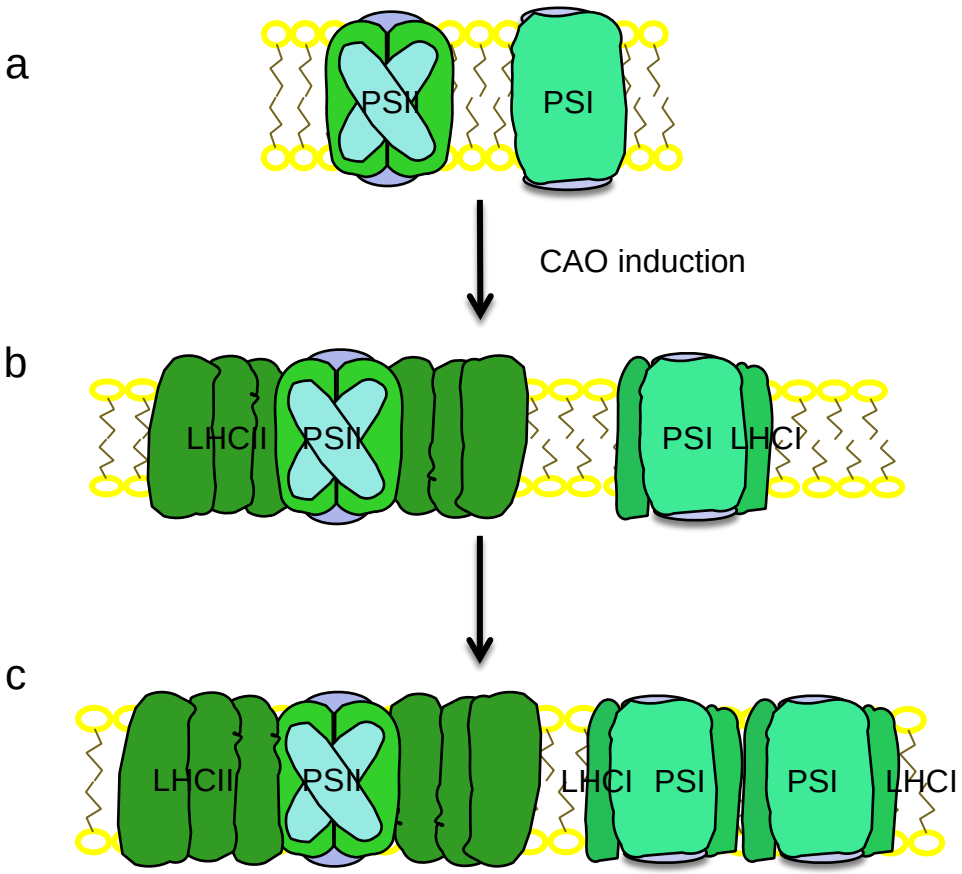

Fig. 9 Working model of PSI and II after CAO induction. a Primary distribution of PSI and PSII in ch1-1 mutants before CAO induction. b After CAO was induced, LHCs assembled with PSI and PSII. Respectively, to form peripheral antenna and the peripheral antenna of PSII was larger than that of PSI. c To balance PSI and PSII excitation, there was an increase in PSI.

Table 1 Chlorophyll content and chlorophyll *a*/*b* ratio in WT plants and transformants

		Chl *a* (nmol/gFW)	Chl *b* (nmol/gFW)	Chl *a*/Chl *b*
WT		1365.5 ± 54.0	406.0 ± 9.5	3.4 ± 0.1
Dex 0 d	6	983.4 ± 62.2	0.0	n.d.[a]
	15	921.6 ± 37.5	0.0	n.d.
	16	724.7 ± 51.9	0.0	n.d.
Dex 4 d	6	1102.0 ± 64.5	196.1 ± 15.2	5.6 ± 0.4
	15	1024.1 ± 39.2	127.4 ± 58.6	9.8 ± 5.8
	16	964.2 ± 82.8	72.1 ± 8.8	13.6 ± 2.8

[a] n.d. stands for not determined.

Supplemental Figure 1

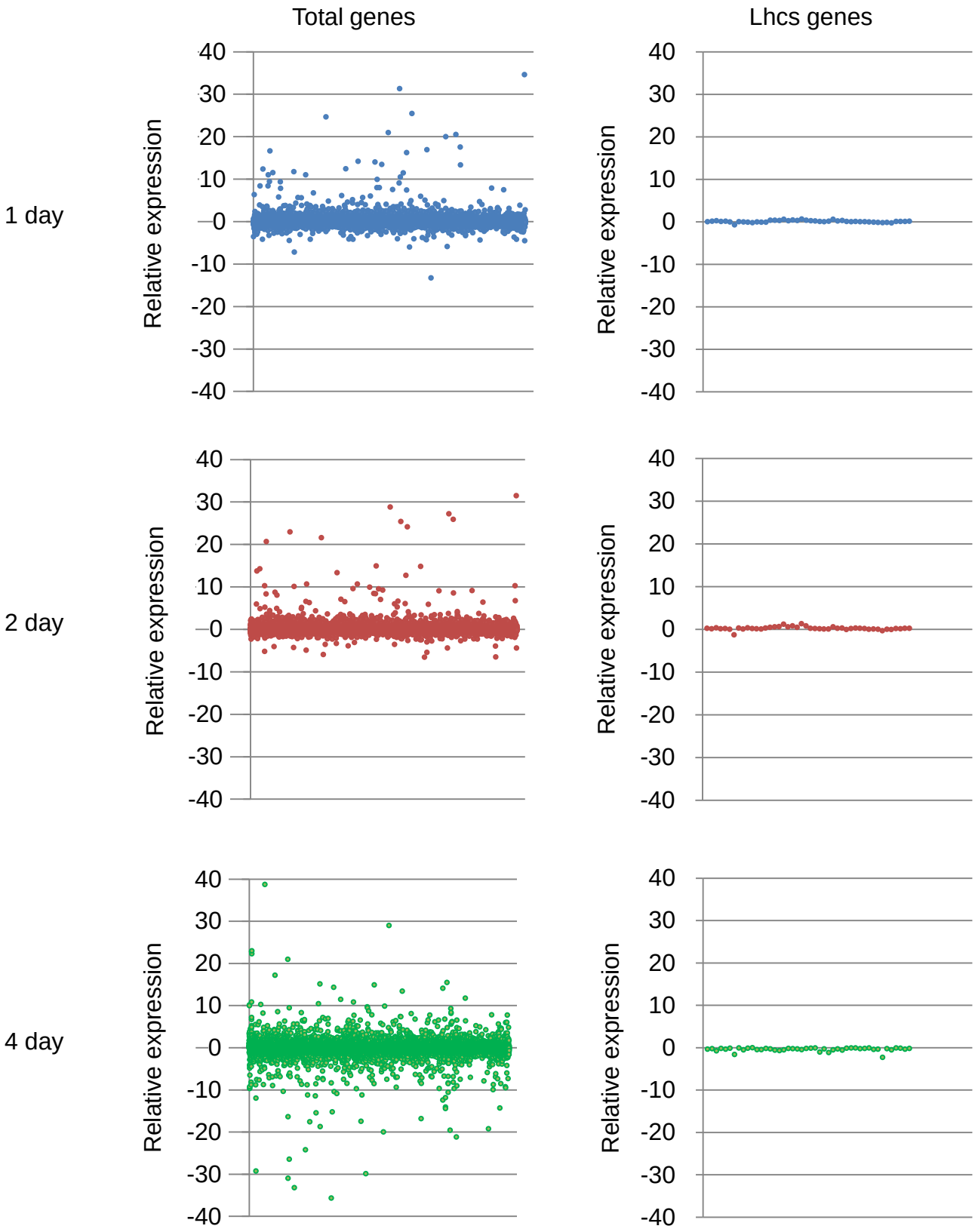

Supplemental Figure 1. Analysis of gene expression. Total RNA was extracted from fully expanded rosette leaves. An untreated sample was used as a control. Each dot corresponds to a gene on microarray.

Supplemental Figure 2

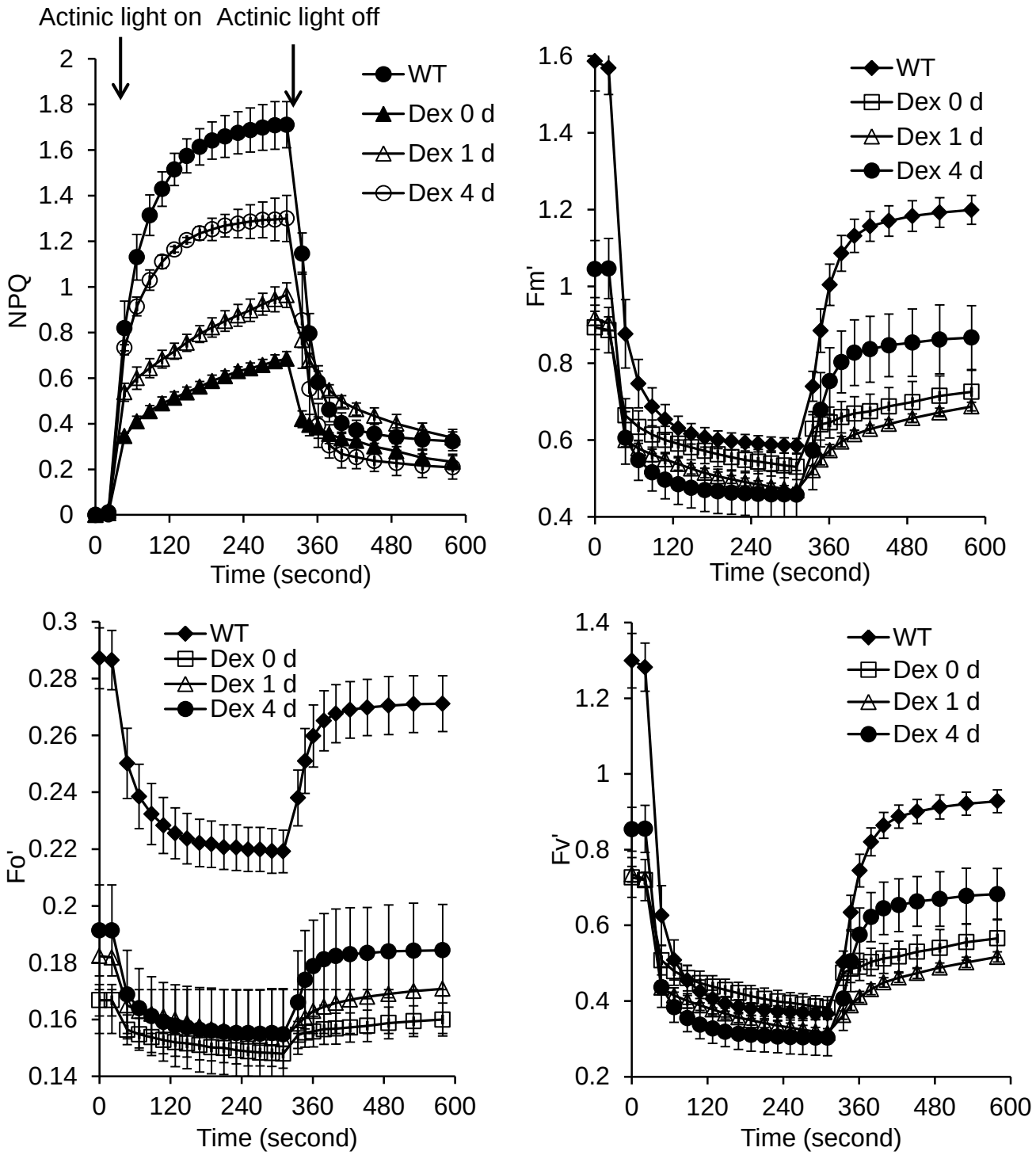

Supplemental Fig. 2 Time course of non-photochemical quenching (qE type), Fo', Fm', and Fv'. Fully expanded leaves from WT and Dex treated and untreated *CAO*/*ch1-1* plants were incubated in the dark for 15 min. NPQ, Fm', Fo', and Fv' were then examined using the PAM system. Error bars represents ± SD (n = 3). Similar results were obtained from three independent experiments.